JACS
JOURNAL OF THE AMERICAN CHEMICAL SOCIETY
Article
pubs.acs.org/JACS

Copper(II) Anilides in sp^3 C-H Amination

Eun Sil Jang,[†,‡] Claire L. McMullin,[§,#] Martina Käß,[∥] Karsten Meyer,[∥] Thomas R. Cundari,*[,§] and Timothy H. Warren*[,†,‡]

[†]Department of Chemistry, Georgetown University, Box 571227-1227, Washington, D.C. 20057, United States

[‡]Department of Chemistry, Purdue University, 560 Oval Drive, West Lafayette, Indiana 47907, United States

[§]Department of Chemistry, Center for Advanced Scientific Computing and Modeling (CASCaM), University of North Texas, Denton, Texas 76203, United States

[∥]Department of Chemistry and Pharmacy, Friedrich-Alexander-University Erlangen-Nuremberg, Egerlandstrasse 1, 91058 Erlangen, Germany

Supporting Information

ABSTRACT: We report a series of novel β-diketiminato copper(II) anilides [Cl$_2$NN]Cu-NHAr that participate in C-H amination. Reaction of H$_2$NAr (Ar = 2,4,6-Cl$_3$C$_6$H$_2$ (Ar^{Cl3}), 3,5-(CF$_3$)$_2$C$_6$H$_3$ (Ar^{F6}), or 2-py) with the copper(II) *t*-butoxide complex [Cl$_2$NN]-Cu-^{t}OBu yields the corresponding copper(II) anilides [Cl$_2$NN]-Cu-NHAr. X-ray diffraction of these species reveal three different bonding modes for the anilido moiety: κ^1-N in the trigonal [Cl$_2$NN]Cu-NHAr^{Cl3} to dinuclear bridging in {[Cl$_2$NN]Cu}$_2$(μ-NHAr^{F6})$_2$ and κ^2-*N,N* in the square planar [Cl$_2$NN]Cu(κ^2-NH-2-py). Magnetic data reveal a weak antiferromagnetic interaction through a π-stacking arrangement of [Cl$_2$NN]Cu-NHAr^{Cl3}; solution EPR data are consistent with monomeric species. Reaction of [Cl$_2$NN]Cu-NHAr with hydrocarbons R-H (R-H = ethylbenzene and cyclohexane) reveals inefficient stoichiometric C-H amination with these copper(II) anilides. More rapid C-H amination takes place, however, when ^{t}BuOO^{t}Bu is used, which allows for HAA of R-H to occur from the ^{t}BuO$^\bullet$ radical generated by reaction of [Cl$_2$NN]Cu and ^{t}BuOO^{t}Bu. The principal role of these copper(II) anilides [Cl$_2$NN]Cu-NHAr is to capture the radical R$^\bullet$ generated from HAA by ^{t}BuO$^\bullet$ to give functionalized aniline R-NHAr, resulting in a novel amino variant of the Kharasch−Sosnovsky reaction.

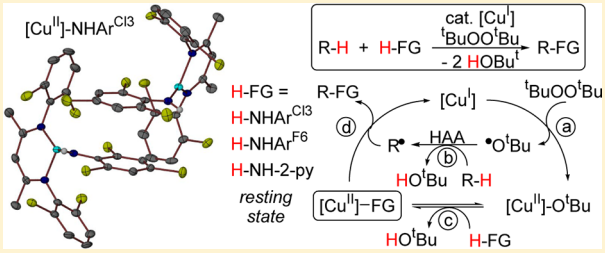

INTRODUCTION

C-H amination allows the construction of C-N bonds directly from C-H bonds and leads to rapid incorporation of N atoms into molecules.[1,2] This reaction proceeds in fewer reaction steps and with lower potential environmental impact as compared to traditional functional group manipulations. Perhaps the best studied sp^3 C-H amination systems involve metal-nitrenes [M] = NR′ (Scheme 1).[3] These reactions produce secondary amines (amides) R-NHR′ employing iminoiodinanes PhI=NR′[4] or in some cases organoazides N$_3$R′.[5−7] Alternatively, Lebel and co-workers have used *N*-tosyloxycarbamates that provide nitrene-like reactivity.[8] While dirhodium or ruthenium catalysts are common, catalyst systems based on Earth abundant metals such as Mn,[9] Fe,[10,11] Co,[12] and Cu[6,7,13] may also be employed.

Scheme 1. C-H Amination: Nitrene and Amide Intermediates

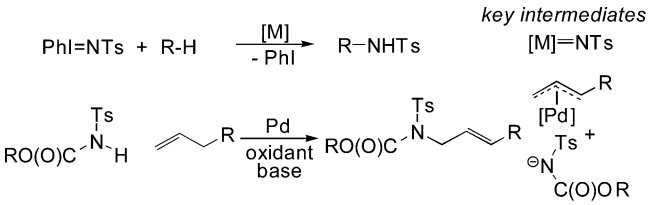

General non-nitrene routes involving metal-amide ([M]-NRR′) intermediates are potentially more versatile and would allow for the construction of both 2° and 3° amines from C-H substrates R-H when 1° (H$_2$NR′) and 2° (HNR^{1}R^2) amine reagents are employed. For instance, White and Liu illustrated the formation of linear amines from terminal alkenes using a Pd-catalyzed protocol with *N*-tosylcarbamates HN(Ts)C(O)-OR.[14] C-H activation provides a Pd(II) π-allyl intermediate subject to intermolecular attack by a mildly basic amide anion such as [N(SO$_2$Ph)C(O)OMe]$^-$. Other mildly basic 2° amines such as HNPh$_2$ may be similarly employed for allylic C-H amination.[15] Other Pd-catalyzed variations take advantage of directed C-H activation to give amide-aryl intermediates subject to C−N reductive elimination such as in the synthesis of carbazoles.[16] Additionally, peroxides have been used as oxidants for sp^3 C-H amination with electron-poor nitrogen sources such as organic amides.[17,18] In some cases, peroxycarbamates ROOC(O)NHR could be directly employed with metal amides [Cu^{II}]-NHR suggested as intermediates.[19]

Received: March 26, 2014
Published: June 18, 2014

 © 2014 American Chemical Society

A common limitation to many C-H amination systems is the requirement for electron-deficient N-substituents in both the nitrene and non-nitrene protocols. While C-H amination has been used in complex molecule synthesis,[2,20] often these electron-withdrawing N-based activating groups (e.g., sulfonyl, carbamoyl) require deprotection and refunctionalization for the synthesis of new alkyl- and aryl-amines via C-H functionalization. This detracts from the potential atom economy that C-H amination can offer. Notable exceptions are reactions that make use of organoazides and proceed via Fe[10] and Cu[7,21] alkyl- or aryl-nitrene intermediates as well as net C-H amination of carbonyl α-C-H bonds with 2° amines via α-C-Br carbonyl intermediates formed upon bromination of carbonyl substrates with $CuBr_2$.[22]

To expand the range of amine coupling partners in C-H functionalization reactions, we recently reported a novel Cu-based catalyst system that employs 1° and 2° alkyl- and arylamines with the mild oxidant $^tBuOO^tBu$.[23,24] Strong C-H bonds such as those in cyclohexane may be efficiently functionalized with amines such as H_2NAd and H_2NAr^{Cl3} (Ar^{Cl3} = 2,4,6-trichloroaniline, Ad = 1-adamantyl) while secondary amines such as morpholine and *N*-methylaniline may also be used (Schemes 2 and 3a).

Scheme 2. Catalytic Cycle for Amination with Alkylamines

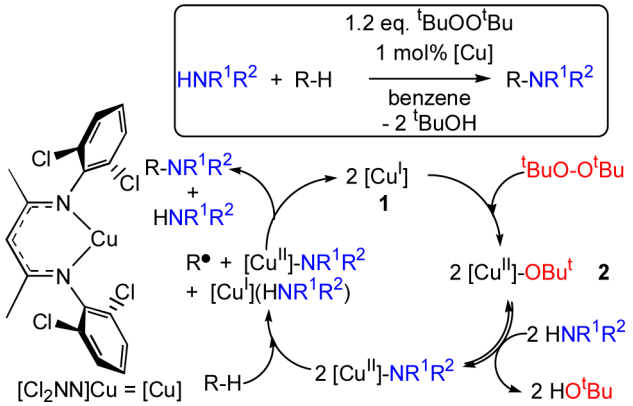

Scheme 3. C-H Amination with Aromatic Amines

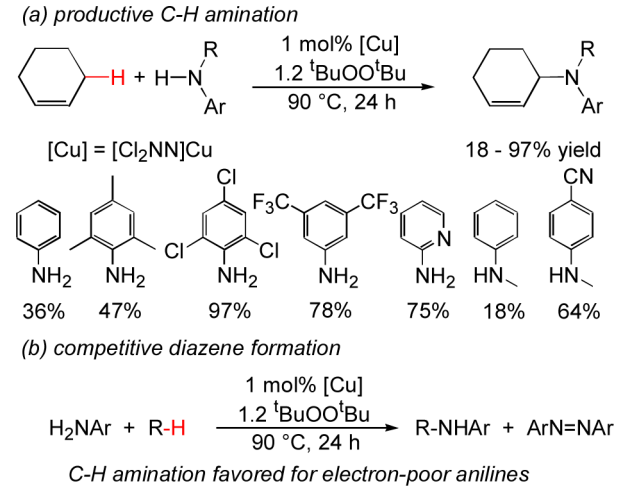

Catalytic reactivity studies of $[Cl_2NN]Cu$ (**1**) with H_2NAd and $^tBuOO^tBu$ informed by the isolation and reactivity of the copper(II) alkoxide $[Cl_2NN]Cu\text{-}O^tBu$ (**2**) and amide $[Cl_2NN]Cu\text{-}NHAd$ (**3**) led to the development of a catalytic cycle that features copper(II) amides $[Cu^{II}]\text{-}NR^1R^2$ as key intermediates (Scheme 2).[23] The copper(I) β-diketiminate $[Cl_2NN]Cu$ (**1**) reacts with $^tBuOO^tBu$ to give the copper(II) alkoxide $[Cl_2NN]Cu\text{-}O^tBu$ (**2**), which undergoes reversible exchange with H_2NAd (K_{eq} = 4(1) in benzene) to give the copper(II) amide $[Cl_2NN]Cu\text{-}NHAd$ (**3**). This three coordinate amido complex stoichiometrically aminates hydrocarbons such as ethylbenzene and indane. Kinetic studies demonstrated that the rate limiting step is H atom abstraction of R-H by $[Cu^{II}]\text{-}NHAd$ to give a radical $R^\bullet$ that may rapidly combine with an additional equivalent of $[Cl_2NN]Cu\text{-}NHAd$ to give the functionalized amine R-NHAd. The HAA step proceeds at modest rates with benzylic substrates. Activation parameters $\Delta H^\ddagger$ = 11.4(4) kcal/mol, $\Delta S^\ddagger$ = −38.7(14) eu, and $\Delta G^\ddagger$(298K) = 22.9(8) kcal/mol were obtained in the stoichiometric reaction of **3** with indane. DFT analysis predicts a modest N-H bond strength of 68 kcal/mol for $[Cl_2NN]Cu\text{-}(NH_2Ad)$ corresponding to an uphill HAA step that contributes to the large KIE in the C-H amination of ethylbenzene (k_H/k_D = 70(9)).[23]

C-H amination with anilines revealed that oxidation of the aniline H_2NAr to diazenes ArN═NAr competes with successful C-H amination (Scheme 3b).[24] Nonetheless, C-H amination may compete successfully with diazene formation, particularly for electron-poor anilines, to give high yields of C-H amination products with substrates such as ethylbenzene or cyclohexene.

To provide a more concrete mechanistic foundation for C-H amination with anilines employing the $[Cl_2NN]Cu$ catalyst, we targeted the synthesis of the anticipated copper(II) anilide intermediates $[Cl_2NN]Cu\text{-}NHAr$. Based on their disinclination to diazene formation, we synthetically target copper(II) anilide intermediates based on electron-poor anilines for our studies. Herein, we discuss their synthesis, structures, and reactivity in the context of catalytic C-H amination. Calculations at the hybrid ONIOM(BP86/6-311+G(d):UFF) level of theory have also been completed to examine the reactivity of copper(II) anilides and elucidate experimental observations.

■ RESULTS AND DISCUSSION

Synthesis and Structure of Copper(II) Anilides. The reaction of $[Cl_2NN]Cu\text{-}O^tBu$ (**2**) with electron-deficient anilines H_2NAr at RT in ether provides copper(II) anilides that may be obtained from ether/pentane as crystals in moderate yields (Scheme 4). For instance, blue crystals of $[Cl_2NN]Cu\text{-}NHAr^{Cl3}$ (**4**) are obtained from ether/pentane at −35 °C in 62% yield. The X-ray structure of **4** reveals two independent molecules featuring three coordinate copper centers (Figure 1). The $Cu\text{-}N_{anilide}$ distances Cu1−N3 and Cu2−N6 of 1.847(3) and 1.841(3) Å are similar to those found in the copper(II) amide $[Cl_2NN]Cu\text{-}NHAd$ (**3**) (1.839(9) Å)[23] and the diphenylamide $[Me_2NN]Cu\text{-}NPh_2$ (1.841(6) Å).[25] These $Cu\text{-}N_{anilide}$ distances may be compared to the somewhat longer $Cu\text{-}N_{\beta\text{-dik}}$ distances [Cu1−N1 1.895(3), Cu1−N2 1.926(3), Cu2−N4 1.893(3), Cu2−N5 1.919(3)]. The $Cu\text{-}N\text{-}C_{ipso}$ angles are each 130.0(2)°, considerably wider than the $Cu\text{-}N_{amide}\text{-}C$ angle in $[Cl_2NN]Cu\text{-}NHAd$ (117.69(11)°).

Perhaps the most striking feature of the X-ray structure of **4** is the interaction of the two crystallographically independent molecules of **4** through a π-stacking interaction (Figure S32 in the Supporting Information). The slightly offset carbon atoms of each N-aryl ring are found separated from their nearest

dx.doi.org/10.1021/ja5026547 | J. Am. Chem. Soc. 2014, 136, 10930−10940

Scheme 4. Synthesis of Copper(II) Anilides 4−6

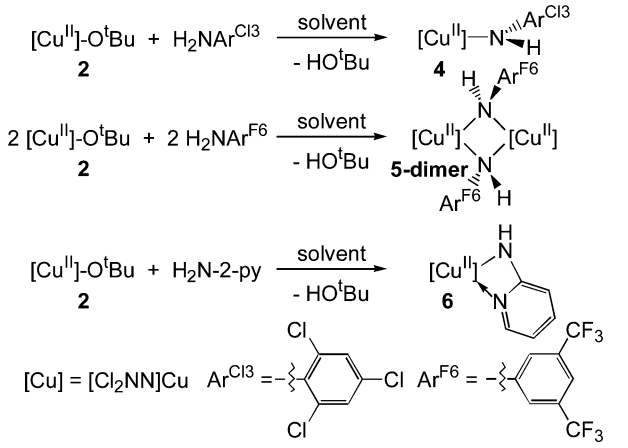

carbon atom in the opposing N-aryl ring within a narrow range (3.443−3.596 Å) with a centroid−centroid distance of 3.470 Å.

The somewhat less sterically hindered, electron-deficient aniline H_2NAr^{F6} reacts to give the corresponding copper(II) anilide that may be isolated as navy blue crystals in 53% yield from pentane. X-ray studies reveal that it exists as the dimer $\{[Cl_2NN]Cu\}_2(\mu\text{-}NHAr^{F6})_2$ (**5-dimer**) in the solid state with the two copper centers separated by 3.102(1) Å (Figure 1). This distorted square planar structure has a twist angle of 27.6° between the $N_{\beta\text{-dik}}$−Cu−$N_{\beta\text{-dik}}$ and $N_{anilide}$−Cu−$N_{anilide}$ planes, possessing a structure reminiscent of the hydroxide bridged dimer $\{[Me_2NN]Cu\}_2(\mu\text{-}OH)_2$ (Cu···Cu = 3.05 Å).[26] The bridging Cu−$N_{anilide}$ distances are ca. 0.2 Å longer than those in monomeric **4** with distances that span 2.035(16)−2.0448(18) Å. The $N_{anilide}$ atoms are separated by 2.650 Å.

Reaction of 2-aminopyridine with **2** in ether leads to a green solution from which green needles of $[Cl_2NN]Cu(\kappa^2\text{-NH-2-py})$ (**6**) may be isolated in 25% yield. Though monomeric, it exhibits a square planar structure due to the κ^2-amidopyridine interaction[27] with Cu−$N_{anilide}$ and Cu−N_{py} distances of 1.975(2) and 2.102(2) Å, respectively (Figure 1). The Cu−$N_{\beta\text{-dik}}$ distances are 1.944(2) and 1.948(2) Å.

Magnetic Behavior of the Copper(II) Anilides. Prompted by the interesting π-stacking interaction between the two anilido rings in the X-ray structure of $[Cl_2NN]Cu\text{-}NHAr^{Cl3}$ (**4**), we undertook a magnetic investigation of these copper anilides in the solid state. Figure 2 shows plots of μ_{eff} vs T for compounds **4**−**6**. Based on the dimeric X-ray structures of **4** and **5**, molecular weights in the calculations of the magnetic data were based on the dimeric compounds. For compound **4**, $\mu_{eff} \approx 2.5\ \mu_B$, which is essentially the spin-only value of 2.45 μ_B expected for two unpaired electrons per dimeric unit. A sharp drop in μ_{eff} at temperatures lower than 50 K is indicative of antiferromagnetic coupling. Modeling these magnetic data with the Hamiltonian $\hat{H} = -2JS_1S_2$ and the g value of 2.09, taken from EPR data (see below), gives a good fit from which $J_{12} = -10.3\ cm^{-1}$ is derived. Thus, at low temperature the two copper centers couple antiferromagnetically, likely mediated by the π-stacked arene rings in **4**. The solid state magnetic data for compounds **5-dimer** and **6** are less remarkable. The magnetic moment at RT for **5-dimer** is 2.55 μ_B and exhibits ferromagnetic coupling of 56 cm^{-1}, whereas mononuclear **6** behaves like a simple Curie paramagnet with a nearly temperature independent magnetic moment of μ_{eff} = 1.75 μ_B, close to the expected spin-only value of 1.73 μ_B for a Cu^{II}, $S = 1/2$ system.

Solution Studies: EPR and UV−Vis Spectroscopy. EPR spectra of **4**−**6** at room temperature in toluene solution are consistent with monomeric $[Cl_2NN]Cu\text{-}NHAr$ species. The EPR spectra of both **4** and **5** at RT each give a broad resonance at g_{iso} = 2.09 and 2.083, respectively, with little resolvable fine structure (Figures S22 and S24 in the Supporting Information). The lack of distinguishable Cu hyperfine structure ($I = 3/2$ for $^{63/65}Cu$) indicates rapid relaxation. This is likely due to facile spin−spin exchange via transient dimeric species $\{[Cl_2NN]Cu\text{-}NHAr\}_2$ with interactions related to those seen in the solid state structures for **4** and **5**. Alternatively, each may possess an intrinsically broad line width at room temperature. In contrast, Cu hyperfine and N superhyperfine coupling is apparent in the RT solution EPR spectra of $[Cl_2NN]Cu(\kappa^2\text{-NH-2-py})$, though significant broadening is also apparent (Figure S26 in the Supporting Information).

Frozen glass spectra of **4**−**6** at 80 K (Figure 3) are each pseudoaxial with g_1 (e.g., g(par)) ranging from 2.18 to 2.21, similar to that found for $[Cl_2NN]Cu\text{-}NHAd$ and $[Me_2NN]Cu\text{-}NPh_2$ (Table 1). The similarity of EPR spectra of **4** and **5** suggests that $[Cl_2NN]Cu\text{-}NHAr^{F6}$ exists in appreciable amounts as its monomer in solution. Nonetheless, the square planar nature of $[Cl_2NN]Cu(\kappa^2\text{-NH-2-py})$ leads to a much

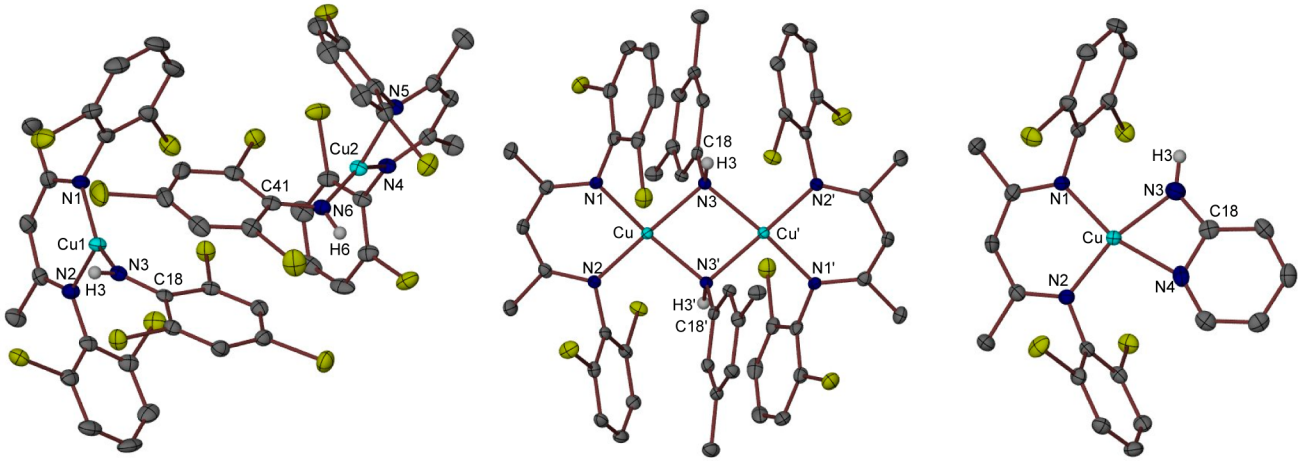

Figure 1. X-ray structures of $[Cl_2NN]Cu\text{-}NHAr^{Cl3}$ (**4**), $\{[Cl_2NN]Cu\}_2(\mu\text{-}NHAr^{F6})$ (**5-dimer**), and $[Cl_2NN]Cu(\kappa^2\text{-NH-2-py})$ (**6-κ^2**).

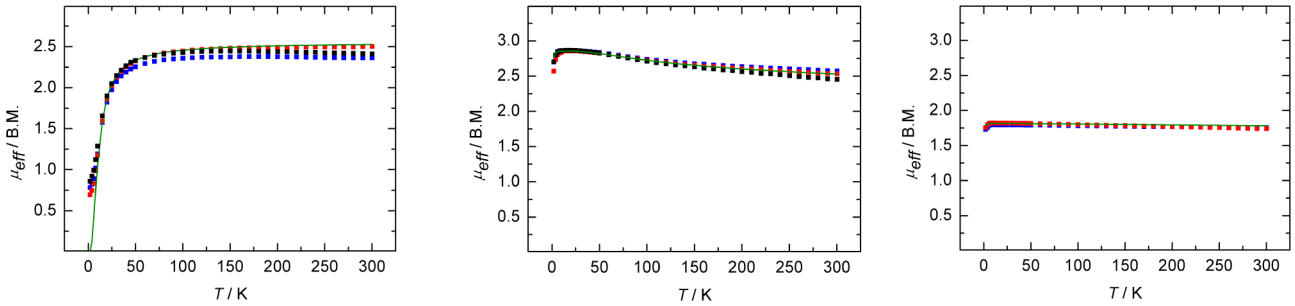

Figure 2. Variable temperature SQUID magnetization data for copper(II) anilides **4**–**6** from 2 to 300 K with an applied field of 1 T (three independent samples each). Data are corrected for underlying diamagnetism, and simulation gives the following parameters: **4**, μ_{eff} (RT) = 2.42 μ_B, J_{12} = −10.3 cm^{-1}; **5**, μ_{eff} (RT) = 2.55 μ_B, J_{12} = 56 cm^{-1}, tip = −150 × 10^{-6}; **6**, μ_{eff} (RT) = 1.75 μ_B, tip = −54.4 × 10^{-6} (tip = temperature independent paramagnetism).

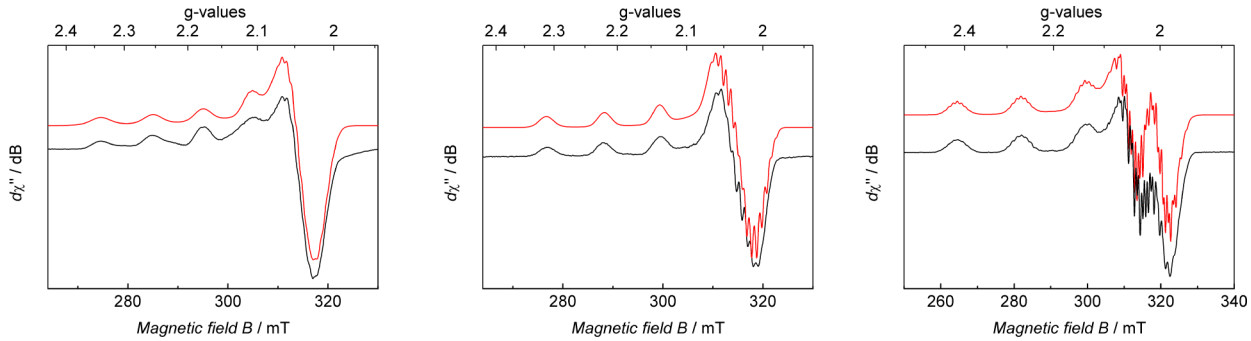

Figure 3. Frozen toluene glass EPR spectra of **4**–**6** at 85 K. Full simulation parameters may be found in Figures S15, S17, and S19 in the Supporting Information.

Table 1. EPR Parameters for Compounds

compound	g_{iso}	g_1	A_1(Cu) (MHz)
[Cl$_2$NN]Cu-O^{t}Bu (**3**)	2.11(1)	2.243(5)	353(10)
[Cl$_2$NN]Cu-NHAd (**1**)	2.067(2)	2.133(5)	365(10)
[Cl$_2$NN]Cu-NHAr^{Cl3} (**4**)	2.090(2)	2.208(5)	288(5)
[Cl$_2$NN]Cu-NHAr^{F6} (**5**)	2.083(2)	2.180(5)	314(5)
[Cl$_2$NN]Cu-NH-2-py (**6**)	2.101(2)	2.201(2)	535(5)
[Me$_2$NN]Cu-NPh$_2$	2.071(3)	2.146(3)	298(5)
[Me$_2$NN]Cu−I	2.104(2)	2.175(2)	410(5)

larger A_1(Cu) = 590 MHz that distinguishes it from the trigonal species with A_1(Cu) in the range 280–370 MHz. Such large A_1(Cu) are typical for square planar Cu(II) complexes.[28] Closer inspection reveals that A_1(Cu) for the trigonal anilido complexes is noticeably less than that for the alkylamide [Cl$_2$NN]Cu-NHAd or the alkoxide [Cl$_2$NN]Cu-O^{t}Bu.[23] This is likely a result of the ability of the unpaired electron density in [Cl$_2$NN]Cu-N(R)Ar species to delocalize over the N-aryl ring (Figure 4).

The UV–vis spectra of copper(II) anilides **4** and **5** are very similar, suggesting that in solution **5** is essentially dissociated to monomeric [Cl$_2$NN]Cu-NHAr^{F6}. Each complex exhibits two low energy optical bands between 700 and 900 nm with high molar absorptivities (3000–5000 M^{-1} cm^{-1}) in aromatic solvents such as ethylbenzene (Table 2). The solution spectra of **4** and **5** are similar to that of [Me$_2$NN]Cu-NPh$_2$, which has two low energy bands at 774 nm (1200 M^{-1} cm^{-1}) and 908 nm (1200 M^{-1} cm^{-1}) that were attributed to Cu–N$_{amide}$ σ–π^* and π–π^* transitions, respectively.[25] Furthermore, cryoscopic

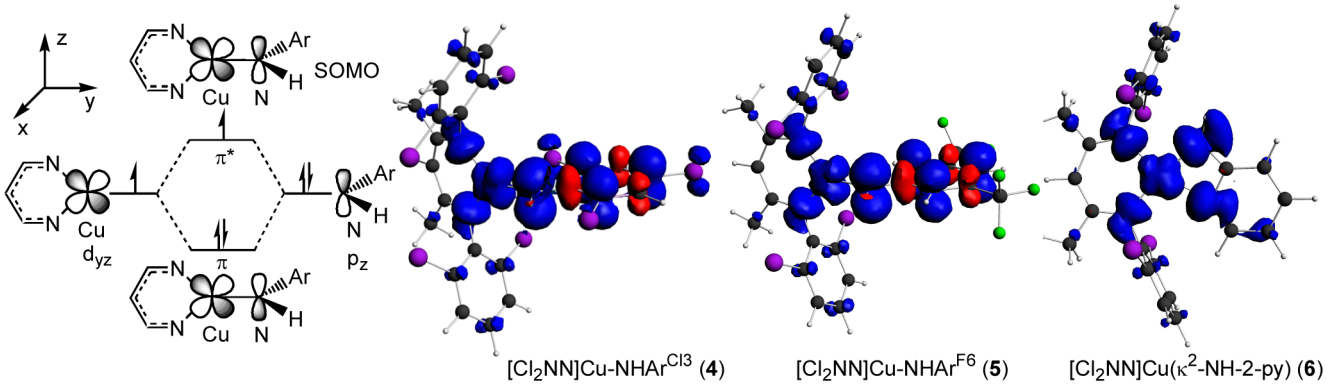

Figure 4. Electronic structure of mononuclear copper(II) anilides with spin density plots for **4**–**6** (ADF2007.1/ZORA/BP/TZ2P(+); excess spin α (blue), spin β (red)).

Table 2. Optical Spectral Bands for Copper(II) Anilides (Ethylbenzene, RT)

compound	λ_1 (nm) (M^{-1} cm^{-1})	λ_2 (nm) (M^{-1} cm^{-1})
$[Cl_2NN]Cu\text{-}NHAr^{Cl3}$ (**4**)	741 (4500)	883 (4200)
$[Cl_2NN]Cu\text{-}NHAr^{F6}$ (**5**)	726 (3700)	863 (3000)
$[Cl_2NN]Cu(\kappa^2\text{-NH-2-py})$ (**6**)	663 (230)	766 (190)
$[Me_2NN]Cu\text{-}NPh_2$	774 (1200)	908 (1200)

molecular weight measurements of **5** indicate a monomeric solution structure in cyclohexane; the UV−vis spectrum of **5** in cyclohexane is closely related to spectra taken in ethylbenzene (Figures S3 and S4 in the Supporting Information). In contrast, the optical spectrum of square planar $[Cl_2NN]Cu\text{-NH-2-py}$ (**6**) possesses two bands at higher energy (660 and 760 nm) but of much lower intensity (ε = 230 and ∼200 M^{-1} cm^{-1}, respectively).

Solutions of the copper(II) anilides may be prepared in essentially quantitative yield by reaction of $[Cl_2NN]Cu\text{-}O^tBu$ (**3**) with H_2NAr. Monitoring the course of reaction by UV−vis in benzene solutions with 0.5 mM concentrations of **3**, the band of the alkoxide at λ_{max} = 471 nm converts cleanly to the corresponding bands of the respective copper(II) anilides **4**−**6** (Scheme 4; Figures S6−S8 in the Supporting Information).

Electronic Structure. DFT (ONIOM(BP86/6-311+G-(d):UFF) methods were used to optimize the geometries and analyze the electronic structures of the monomeric trigonal Cu^{II}-anilide complexes. Both $[Cl_2NN]Cu\text{-}NHAr^{Cl3}$ (**4**) and $[Cl_2NN]Cu\text{-}NHAr^{F6}$ (**5-mono**) possess an electronic structure similar to that discussed for the similar alkylamide $[Cl_2NN]Cu\text{-}NHAd$ (**3**)[23] and anilide $[Me_2NN]Cu\text{-}NPh_2$.[25] Prominent in these trigonal copper(II)-amides is the 2-center, 3-electron π-interaction between the formally d^9 Cu^{II} center and the lone pair of an anionic sp^2-hybridized $N_{anilide}$ donor (Figure 4). The high covalency of this interaction leads to significant delocalization of the unpaired electron formally ascribed to the d^9 Cu^{II} center onto the anilido N atom and indeed into the anilido aromatic ring. The planar $N_{anilide}$ atom along with the orthogonal orientation of the anilido aromatic ring orthogonal to the β-diketiminato backbone allows for the anilido π-system to efficiently participate in this interaction. TD-DFT (ADF 2007.1 ZORA/BP/TZ2P(+)) calculations suggest that the two low energy optical transitions observed each for mononuclear, trigonal **4** and **5** correspond to $Cu\text{−}N_{amide}$ $\sigma\text{−}\pi^*$ and $\pi\text{−}\pi^*$ transitions (Tables S6−S9 and Figures S41, S43, S45, and S47 in the Supporting Information). In particular, the lowest energy optical absorptions correspond to clean $\pi\text{−}\pi^*$ transitions (Figure 4) as found for the related diphenylamide complex $[Me_2NN]Cu\text{-}NPh_2$.[25]

The square planar complex $[Cl_2NN]Cu(\kappa^2\text{-NH-2-py})$ (**6-κ^2**) possesses an electronic structure that is more typical of square planar Cu(II) species. Consistent with its large A_1(Cu) = 535(5) MHz, there is considerably more unpaired electron density at Cu in **6-κ^2** (0.45 e^-) than in trigonal **3**−**5** (0.31−0.36 e^-) and the putative κ^1-N isomer of **6** (**6-κ^1**) (0.38 e^-). Moreover, the remaining unpaired electron density in **6-κ^2** is spread more evenly among the 4 N donor atoms whereas in trigonal **3**−**5** and **6-κ^1** the amido N atom possesses considerably more spin density than the β-diketiminato N-donors (Table 3).

Catalytic C-H Amination of Ethylbenzene and Cyclohexane with Electron-Poor Anilines. The isolation of the copper(II) anilides **4**−**6** offers an opportunity to examine the roles that copper(II) anilides $[Cl_2NN]Cu\text{-}NHAr$ play in C-H amination. Each of the corresponding anilines, H_2NAr, employed in this study serves as an efficient coupling partner in C-H amination with ethylbenzene and cyclohexane under catalytic conditions using $^tBuOO^tBu$ as a substrate with 1 mol % $[Cl_2NN]Cu$ in neat hydrocarbon solvent (Scheme 5). While

Table 3. Spin Densities (e^-) in Copper(II) Amido Complexes (ADF2007.1/ZORA/BP/TZ2P(+))

compound	Cu	N_{amide}	$N_{\beta\text{-dik}}$
4	0.36	0.23	0.07, 0.13
5-mono	0.36	0.25	0.09, 0.13
6-κ^2	0.45	0.15 (NH)	0.12, 0.14
		0.08 (py)	
6-κ^1	0.38	0.25	0.09, 0.13
3	0.31	0.49	0.08, 0.10

Scheme 5. Catalytic C-H Amination with Electron-Poor Anilines

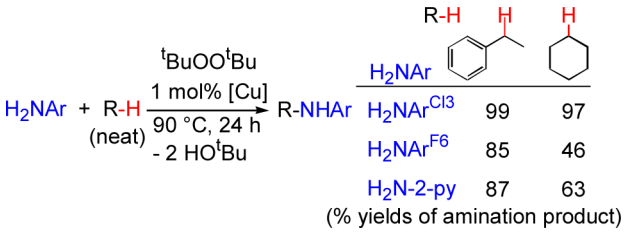

the C-H amination of these two C-H substrates was previously reported with H_2NAr^{Cl3},[24] the two other anilines H_2NAr^{F6} and H_2N-2-py also participate in C-H amination with these two substrates. Higher yields are observed with neat ethylbenzene (85−99%) than cyclohexane (46−97%) attributed to the lower C-H bond strength of ethylbenzene (87 kcal/mol)[29] vs cyclohexane (97 kcal/mol).[29]

$[Cl_2NN]Cu\text{-}NHAr^{Cl3}$ (**4**) is clearly present in catalytic C-H amination of ethylbenzene with H_2NAr^{Cl3}. Following a catalytic reaction in neat ethylbenzene by UV−vis spectroscopy in a cuvette thermostated at 80 °C clearly reveals the strong optical bands of **4** at λ = 741 and 883 nm. Based on the amount of catalyst used, we estimate that 70% of the $[Cl_2NN]Cu$ species present exists as $[Cl_2NN]Cu\text{-}NHAr^{Cl3}$ initially, which declines as the reaction nears completion over 5 h (Figure S9 in the Supporting Information).

The direct observation of $[Cl_2NN]Cu\text{-}NHAr$ species **4**−**6** in catalytic C-H amination reactions employing the corresponding anilines H_2NAr begs the question of what role these $[Cu^{II}]\text{-}NHAr$ species may play in the reaction. Aiming at answering this question, we first focused on $[Cl_2NN]Cu\text{-}NHAr^{Cl3}$. Surprisingly, this copper(II) anilide is rather stable in neat ethylbenzene at 80 °C. Preliminary kinetic analysis suggests slow, second-order decay of $[Cu^{II}]\text{-}NHAr^{Cl3}$ in neat ethylbenzene with a half-life of ca. 11 h (initial concentration = 0.40 mM; Figure S10 in the Supporting Information). After the sample has completely bleached (40 h), analysis of the mixture by GC−MS revealed that only 20% of the C-H amination product was present; the remainder is H_2NAr^{Cl3}. Based on the stoichiometry observed in the C-H amination of ethylbenzene by isolated $[Cl_2NN]Cu\text{-}NHAd$ (**1**), which proceeds via smooth pseudo first-order decay of **1** in excess ethylbenzene at 25 °C,[23] we anticipate a maximum yield of 50% conversion of $[Cl_2NN]Cu\text{-}NHAr^{Cl3}$ (**4**) to the C-H amination product

dx.doi.org/10.1021/ja5026547 | J. Am. Chem. Soc. 2014, 136, 10930−10940

PhCH(NHAr^{Cl3})Me along with an equivalent amount of H_2NAr^{Cl3}. While we observe some C-H amination product from the isolated copper(II) anilides [Cl_2NN]Cu-NHAr (**4**–**6**) (Scheme 6), it is nonetheless clear that the rate and efficiency

Scheme 6. Stoichiometric C-H Amination with Cu-anilides 4-6

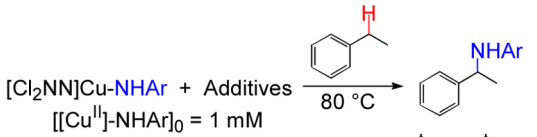

additive(s)	none*	1/2 $^tBuOO^tBu$	1/2 $^tBuOO^tBu$ + 10 mol% [Cu^I]
Cu-anilide	% yield of PhCH(NHAr)Me		
[Cu^{II}]-NHAr^{Cl3} (**4**)	10	82	91
[Cu^{II}]-NHAr^{F6} (**5**)	0	94	96
[Cu^{II}]-NH-2-py (**6**)	1	62	62

* max yield = 50%

of stoichiometric C-H amination is not commensurate with that observed in the catalytic variant employing H_2NAr with 1.2 equiv of $^tBuOO^tBu$ in the presence of 1 mol % [Cu] (Scheme 5).

Since it appears that [Cl_2NN]Cu-NHAr species are not particularly efficient at functionalizing neat ethylbenzene by themselves, we considered an alternative reagent for HAA: the $^tBuO^\bullet$ radical (Scheme 7). We recently demonstrated that the

Scheme 7. C-H Amination via HAA by $^tBuO^\bullet$ radical

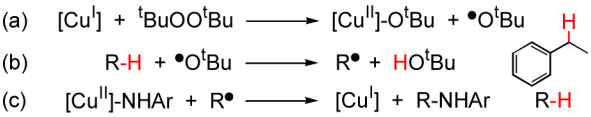

reaction of [Cl_2NN]Cu with $^tBuOO^tBu$ in an inert solvent (fluorobenzene) proceeds readily via overall second order kinetics (rate = k[Cu^I][$^tBuOO^tBu$]) with a rate constant of 5.9(2) M^{-1} s^{-1} at 20 °C consistent with generation of the $^tBuO^\bullet$ radical (Scheme 7a).[30] In addition, use of dicumylperoxide ($PhMe_2COOCMe_2Ph$) led to increased amounts of acetone formation as the [Cu^I] concentration decreased, providing firm evidence for the production of the cumyloxy radical $PhMe_2CO^\bullet$ that rapidly decays by β-scission to give acetophenone and $Me^\bullet$. Furthermore, $^tBuOO^tBu$ reacts with [Cu^I] in cyclohexane to give Cy-O^{t}Bu, strongly suggesting that the $^tBuO^\bullet$ radical formed can undergo HAA reactions with strong C-H bonds.[31]

Addition of 1/2 equiv of $^tBuOO^tBu$ to 1 mM solutions of [Cu^{II}]-NHAr in ethylbenzene followed by heating at 80 °C for 24 h led to dramatic increases in the amount of functionalized amine PhCH(NHAr)Me observed (Scheme 5). Following the reaction of [Cu^{II}]-NHAr^{Cl3} (**4**) with $^tBuOO^tBu$ in ethylbenzene at 80 °C by UV–vis reveals zero-order decay of [Cu^{II}]-NHAr^{Cl3} (**4**) coupled to zero-order growth of [Cu^{II}]-O^{t}Bu (**3**) with essentially identical zero-order rate constants (Figure 5). This zero-order decay of **4** coupled with growth of **1** also occurs at 25 °C, albeit more slowly and with an induction period (Figure S11 in the Supporting Information). Following the decay of [Cu^{II}]-NHAr^{Cl3} in the presence of 3–10 equiv of $^tBuOO^tBu$ and 1 equiv of added [Cl_2NN]Cu results in a linear increase of

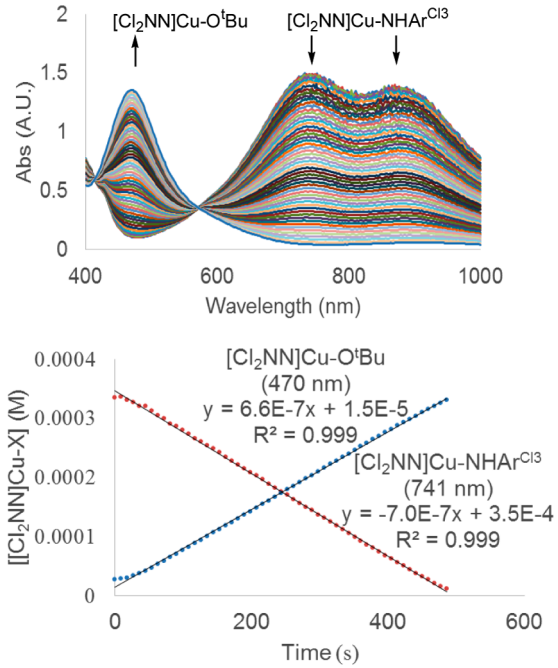

Figure 5. Zero-order decay of [Cl_2NN]Cu-NHAr^{Cl3} (**4**) and zero-order growth of [Cl_2NN]Cu-O^{t}Bu (**1**) in ethylbenzene at 80 °C in the presence of $^tBuOO^tBu$.

the zero-order rate for [Cu^{II}]-NHAr^{Cl3} decay (Figures S13–16 in the Supporting Information), signaling a first-order dependence on [$^tBuOO^tBu$].

The zero-order dependence in [Cu^{II}]-NHAr (**4**) signals that another species is responsible for initiating H atom abstraction of the ethylbenzene C-H substrate. Based on the rapid generation of the $^tBuO^\bullet$ radical from [Cl_2NN]Cu and $^tBuOO^tBu$ (Scheme 7a), we suspect that a small amount of solvent-free copper(I) species [Cl_2NN]Cu generated by slow decay of [Cl_2NN]Cu-NHAr in ethylbenzene is responsible for the formation of $^tBuO^\bullet$ and [Cl_2NN]Cu-O^{t}Bu (**2**) in the reaction of [Cl_2NN]Cu-NHAr^{Cl3} and $^tBuOO^tBu$. Reaction of $^tBuO^\bullet$ with ethylbenzene (R-H) to generate the corresponding ethylbenzene radical ($R^\bullet$) swiftly proceeds (Scheme 7b) followed by capture of the copper anilide [Cl_2NN]Cu-NHAr (**4**) by $R^\bullet$ to give the C-H amination product R-NHAr^{Cl3} (Scheme 7c).

Direct Observation of C–N Bond Formation–Capture of Trityl Radical by [Cu]-NHAr. We took advantage of the ready generation of the trityl radical $Ph_3C^\bullet$ by equilibrium dissociation of Gomberg's dimer {Ph_3C}$_2$ to probe the reactivity of [Cu^{II}]-NHAr species with a C-centered radical under mild conditions. Addition of 1/2 equiv of {Ph_3C}$_2$ to [Cu^{II}]-NH-py (**6**) in benzene-d_6 results in the formation of the corresponding *N*-trityl substituted anilines Ph_3C-NH-2-py and an equivalent of [Cl_2NN]Cu(benzene) each in 78% yield (Scheme 8). While reaction of Gomberg's dimer was not as

Scheme 8. Capture of $Ph_3C^\bullet$ by [Cu^{II}]-NHAr

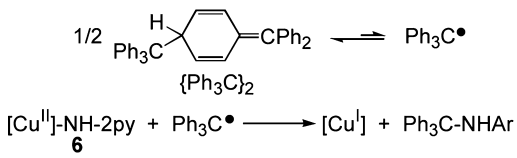

dx.doi.org/10.1021/ja5026547 | J. Am. Chem. Soc. 2014, 136, 10930–10940

clean with the Cu(II) anilides **4** and **5**, this experiment reveals that attack of [Cu^{II}]-NHAr species by radicals $R^{\bullet}$ can deliver the corresponding functionalized amine R-NHAr.

Theory—Formation and Reactivity of Copper(II) Anilides. At the ONIOM(BP86/6-311+G(d):UFF) level of theory, the acid—base exchange reactions between [Cl_2NN]Cu-O^{t}Bu and H_2NAr are computed to be slightly exergonic for differing aryls (Ar); ΔG in kcal/mol = −2.6 (Ar = Ph), −0.4 (Ar = py), −2.4 (Ar = Ar^{Cl3}) and −2.8 (Ar = Ar^{F6}) (Scheme 4). DFT predicts the observed κ^2-NH-2-py coordination observed to be 2.4 kcal/mol lower in free energy than κ^1-NH-2-py coordination to give a trigonal [Cu^{II}]-NHAr species.

The arylamine N—H bond strength in each copper(I) adduct [Cl_2NN]Cu(NH_2Ar) reflects the driving force for HAA by the corresponding copper(II) anilide [Cl_2NN]Cu-NHAr. These N—H bond strengths are calculated to be 48.3, 48.1, and 52.7 kcal/mol for the copper(I) aniline adducts derived from **4**, **5**, and **6**, respectively (Scheme 9). These values for the N—H bond enthalpy are approximately *ca.* 40 kcal/mol lower than that found in the free anilines (exp. 90—95 kcal/mol)[29] calculated to be 89.4, 91.3, and 91.9 kcal/mol for H_2NAr^{Cl3}, H_2NAr^{F6}, and H_2N-2-py, respectively. The modest N—H bond strengths in the copper(I) aniline adducts [Cl_2NN]Cu(NH_2Ar) reflect the relative stabilization of the aminyl radical as copper(II) anilides [Cl_2NN]Cu-NHAr that possess highly delocalized unpaired electron-density (Figure 4, Table 3). Furthermore, the more acidic N—H bond in arylamine adducts [Cl_2NN]Cu(NH_2Ar) as compared to the corresponding alkylamine species [Cl_2NN]Cu(NH_2Ad) may also contribute to lower N—H bond strengths in [Cl_2NN]Cu(NH_2Ar) complexes.[32] These relatively low values of N—H bond strength result in highly endothermic HAA of ethylbenzene by [Cu^{II}]-NHAr species.

Scheme 9. Calculated Thermodynamics for HAA of Ethylbenzene by 4, 5 and 6-κ^1

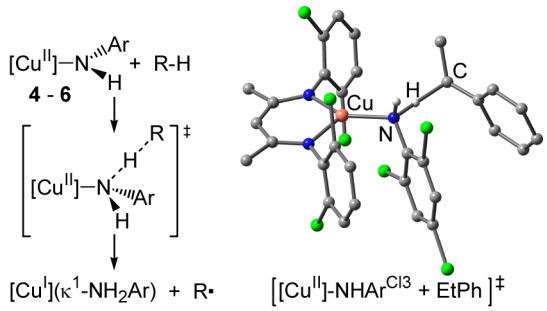

cmpd	N-H BDE	ΔH	ΔG(298 K)	ΔH‡	ΔG‡(298 K)	ΔS‡
4	48.3	34.9	34.1	21.3	34.6	-44.6
5	48.1	35.0	34.9	17.4	30.2	-42.9
6-κ¹	52.7	30.4	31.4	16.8	30.8	-46.7

N-H BDE of [Cu^I](κ^1-NH2Ar), enthalpies, and free energies in kcal/mol; ΔS‡ in cal/mol K

The transition states for HAA of ethylbenzene by [Cu^{II}]-NHAr (Scheme 9) are similar in structure to that found for HAA of indane by [Cl_2NN]Cu-NHAd (**3**), yet importantly are appreciably higher in energy for the anilides **4**—**6**. As a point of comparison, the experimental activation parameters for HAA of indane by **3** closely match those found by theory. ($\Delta H_{exp}^{\ddagger}$ = 11.4(4) kcal/mol and $\Delta S_{exp}^{\ddagger}$ = −38.7(14) e.u. with $\Delta G_{exp}^{\ddagger}$ = 22.9(8) kcal/mol; $\Delta H^{\ddagger}$ = 11.5 kcal/mol, $\Delta S^{\ddagger}$ = −46.8 e.u. with $\Delta G^{\ddagger}$ = 25.2 kcal/mol). On the other hand, the transition states for HAA of ethylbenzene by **4**—**6** are calculated to be much higher in free energy, largely due to increased enthalpies of activation ($\Delta H^{\ddagger}$ = 21.3, 17.4, and 16.8 kcal/mol for **4**, **5**, and **6-κ^1**, respectively). No transition state was identified from the square planar **6-κ^2**, due to the bidentate coordination mode of the amido-2-pyridine substrate. The significant increase in enthalpy of activation does not originate from the C-H substrate since the benzylic C-H bonds of ethylbenzene and indane are of similar strength (calc. BDE = 83.1 (ethylbenzene) vs 83.5 kcal/mol (indane)). Instead, the HAA enthalpies of activation reflect the weaker N—H bonds calculated in the copper(I) aniline adducts [Cu^I](NH_2Ar) (48.1—52.7 kcal/mol) vs the copper(I) amine adduct [Cu^I](NH_2Ad) (68.0 kcal/mol).

On the other hand, HAA of ethylbenzene by the ^{t}BuO$^{\bullet}$ radical is calculated to be highly thermodynamically favorable (ΔG = −15.4 kcal/mol) driven by the strong O—H bond in ^{t}BuO-H (calc: 98.3 and expt: 105 kcal/mol[29]) that leads to kinetically competent HAA of ethylbenzene ($\Delta H^{\ddagger}$ = −1.8 kcal/mol, $\Delta S^{\ddagger}$ = 36.8 e.u. and $\Delta G^{\ddagger}$(298 K) = 9.2 kcal/mol). These values compare well to experimental values for HAA reactions of ^{t}BuO$^{\bullet}$ with related hydrocarbons such as toluene and cyclohexane ($\Delta G^{\ddagger}$(298 K) = 10.2(5) and 9.4(7) kcal/mol, respectively).[31] Thus, generation of the ^{t}BuO$^{\bullet}$ radical would be expected to swiftly yield the 2° benzylic ethylbenzene radical (Scheme 7b).

The radical $R^{\bullet}$ generated via HAA from R-H by ^{t}BuO$^{\bullet}$ conceptually may be captured in two conceptually different ways by the [Cu^{II}]-NHAr intermediates to ultimately give the C-H amination product R-NHAr (Schemes 7 and 10). Capture directly at the copper center would result in the copper(III) organometallic species [Cu^{III}](R)(NHAr), which possess square planar coordination at Cu owing to their d^8 electronic configuration. Direct capture at copper of the 2° benzylic radical $R^{\bullet}$ derived from R-H = ethylbenzene by [Cu^{III}]-NHAr species **4**—**6** is calculated to be nearly thermoneutral (ΔH = +3.7, −1.5, and −4.2 kcal/mol, respectively), but significantly entropically disfavored (ΔS = −57.4, −53.3, −58.7 e.u. at 298 K) rendering capture at Cu endergonic with ΔG values of 20.8, 14.4, and 13.3 kcal/mol at 298 K. Due to the high oxidation state at Cu as well as the crowded square planar environment, reductive elimination to give the corresponding [Cu^I](NH(R)-Ar) adducts containing the coordinated product amine R-

Scheme 10. HAA of R-H by ^{t}BuO$^{\bullet}$ and Radical Capture of $R^{\bullet}$ by Copper(II) Anilides 4—6

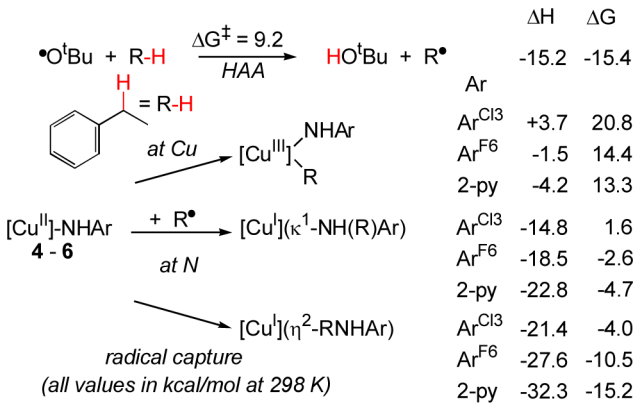

NHAr is favored (Scheme 10). On the other hand, direct reaction of R• at the N atom to give the product amine R-NHAr coordinated to the copper center is much more thermodynamically favorable. Moreover, η^2-bound amine adducts (via the *N*-aryl group) in [Cu^{I}](η^2-ArNHR) species are more thermodynamically stable than the corresponding *N*-bound adducts [Cu^{I}](κ^1-NH(R)Ar). Considering the [Cu^{I}](η^2-ArNHR) complexes, addition of a radical R• to copper(II) anilides **4**−**6** is calculated to be exothermic (ΔH = −21.4, −27.6, and −32.3 kcal/mol, respectively), but significantly entropically disfavored (ΔS = −58.6, −57.3, −57.3 e.u. at 298.15 K). Nonetheless, radical capture at N to give the [Cu^{I}](η^2-ArNHR) adducts is still favorable with ΔG values of −4.0, −10.5, and −15.2 kcal/mol at 298.15 K. While these calculated energetics indicate that radical capture at either Cu or N are each favorable in terms of enthalpy (ΔH), free energy (ΔG) favors radical capture at N due to unfavorable entropy ($T\Delta S$) terms. While direct capture of R• at N is clearly thermodynamically favored (Scheme 10, Figure S36 in the Supporting Information), radical addition reactions to either Cu or N are likely to have low barriers.

■ DISCUSSION AND CONCLUSIONS

The synthesis of copper(II) anilides **4**−**6** allowed a detailed investigation into the mechanism of efficient C-H amination with the corresponding aromatic amines. Copper(II) anilides engage in a diversity of bonding modes including terminal, bridging dinuclear and κ^2-*N*,*N* for the anilide derived from 2-aminopyridine. Based on earlier catalytic C-H functionalization studies, these copper(II) anilides derived from electron-poor anilines appear to be quite stable toward N−N bond formation that could lead to diazenes ArN═NAr, perhaps via coupling of two [Cu^{II}]-NHAr species. While the X-ray structure of [Cl$_2$NN]Cu-NHAr^{F6} clearly illustrates that this species can dimerize, it does so via Cu−N−Cu bridging interactions. The crowded nature of this dimer results in facile formation of monomeric [Cl$_2$NN]Cu-NHAr^{F6} as evidenced by solution EPR and UV−vis studies.

Unlike the alkylamide complex [Cl$_2$NN]Cu-NHAd (**3**), the corresponding anilide complexes **4**−**6** do not engage in efficient HAA reactions with ethylbenzene under mild conditions. Higher temperatures (e.g., 80 °C) are required, and yields of the C-H functionalized amine PhCH(NHAr)Me are low to negligible. In contrast when a [Cu^{I}]/^{t}BuOO^{t}Bu mixture is added to an ethylbenzene solution of **4**, facile conversion takes place, completely consuming the anilide and delivering the functionalized amine R-NHAr in high yield. These studies suggest that ^{t}BuO• is the predominant HAA agent in the efficient C-H amination with anilines, generating the R• radical from R-H which may be captured by [Cu^{II}]-NHAr to give R-NHAr.

This mechanism also extends to C-H amination by alkylamines. Whereas [Cl$_2$NN]Cu-NHAd (**3**) undergoes clean, first-order decay in excess ethylbenzene at 25 °C (rate = k[[Cu^{II}]-NHAd][ethylbenzene], k = 1.51(3) × 10^{-5} M^{-1} s^{-1}; Figure S21 in the Supporting Information) addition of ^{t}BuOO^{t}Bu greatly accelerates the reaction and leads to zero-order decay of **3** (Figure S20 in the Supporting Information). At 0.50 mM initial concentrations of **3** in ethylbenzene the half-life for decay of **3** is 5590 s whereas in the presence of 1.2 equiv of ^{t}BuOO^{t}Bu the initial (zero-order) half-life shortens dramatically to 555 s. Thus, generation of ^{t}BuO• and subsequent HAA of ethylbenzene by ^{t}BuO• successfully competes with slower HAA by [Cl$_2$NN]Cu-NHAd (**3**).

While theoretical studies demonstrate that these three-coordinate copper(II) anilides may participate in HAA reactions with ethylbenzene, they possess rather high barriers with $\Delta G^{\ddagger}$(298 K) = 30−35 kcal/mol depending on the anilide substituent. These barriers are 5−10 kcal/mol higher than established for the copper(II) alkylamide [Cl$_2$NN]Cu-NHAd (**3**).[23] These differences reflect the lower N−H bond strength in the HAA product [Cl$_2$NN]Cu(NH$_2$Ar) as compared to [Cl$_2$NN]Cu(NH$_2$Ad) and track differences in the N−H bond strength in the corresponding free primary amines H$_2$NR. The N−H bond in alkylamines (100 kcal/mol) is generally 5−10 kcal/mol stronger than in anilines (90−95 kcal/mol); electron-deficient aromatic substituents generally enhance the N−H bond strength in anilines.[29] As shown by experiment, capture of the radical R• by [Cu^{II}]-NHAr is facile. Capture at either Cu or N is enthalpically favorable, though the former is endergonic while direct addition to N is favored. Similar trends were found in the thermodynamics of addition of the cyclohexyl radical to [Cu^{II}]-O^{t}Bu that strongly favors formation of the corresponding copper(I) ether adduct [Cu^{I}](Cy(O^{t}Bu)).[30]

Taken together, these studies suggest a catalytic cycle for C-H amination with anilines that is a variation of the Kharasch-Sosnovsky reaction. First reported in 1958, Kharasch and Sosnovsky found that peracetates such as PhC(O)OO^{t}Bu functionalize allylic C-H bonds in substrates R-H to directly form benzoates R−OCH(O)Ph (Scheme 11).[33,34] A variety of simple copper(I) salts such as CuCl serve as catalysts for this reaction at higher temperatures (60−90 °C). Importantly, enantioselective variants have been developed based on cationic copper(I) complexes of bis(oxazolines) and other chiral scaffolds that deliver ee's as high as 96%.[34]

Scheme 11. Kharasch-Sosnovsky Reaction

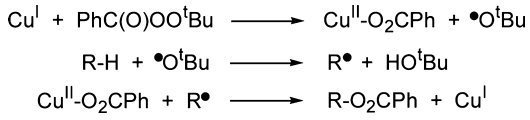

The copper(I) species [Cl$_2$NN]Cu serves two essential roles in C-H functionalization catalysis. It swiftly generates the very reactive ^{t}BuO• radical capable of HAA of R-H (Scheme 12b) upon reaction with ^{t}BuOO^{t}Bu that also provides [Cu^{II}]-O^{t}Bu (**2**) (Scheme 12a). Facile acid/base chemistry between amines H$_2$NR′ (especially electron-poor amines such as anilines) and [Cu^{II}]-O^{t}Bu to generate [Cu^{II}]-NHR represents the second key role for the copper complex (Scheme 12c). Coordination of the

Scheme 12. General C-H Amination via Copper(II) Amides

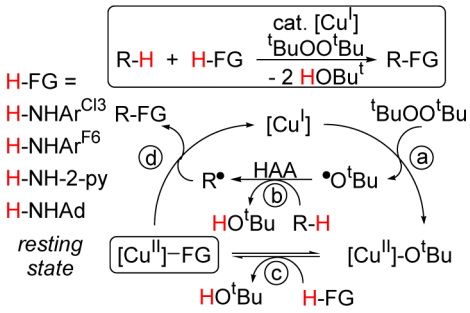

dx.doi.org/10.1021/ja5026547 | J. Am. Chem. Soc. 2014, 136, 10930−10940

amide to the copper center renders the NHR′ moiety particularly reactive toward reaction with C-based radicals R• (Scheme 12d).

These mechanistic studies also open the possibility of employing other functional groups (H-FG) that could undergo facile acid/base exchange with [Cu^{II}]-O^{t}Bu with loss of HO^{t}Bu to give [Cu^{II}]-FG intermediates. Generation of ^{t}BuO• radical (through reaction of [Cu^I] and ^{t}BuOO^{t}Bu)[30] can lead to facile HAA reactions with a wide range of sp^3-hybridized C-H bonds in substrates R-H to give R• under mild conditions with bimolecular rate constants in the range of 10^5 to 10^8 M^{-1} s^{-1}.[31] Reaction of R• with [Cu^{II}]-FG could conceivably deliver new C-H functionalized species R-FG with concomitant reduction of the Cu center to [Cu^I].[35] In fact, Hartwig and co-workers recently found that amidation of unactivated sp^3 C-H bonds can occur with organic amides, ^{t}BuOO^{t}Bu and phenanthroline copper(I) complexes by a related variation of the Kharasch-Sosnovsky reaction in which the ^{t}BuO• radical was also identified as the H atom abstracting reagent.[18] These concepts underscore the possibility of a family of new, mechanistically related C-H functionalization reactions that are under active development in our laboratory.

■ EXPERIMENTAL SECTION

General Procedures. All experiments were carried out in a dry nitrogen atmosphere using an MBraun glovebox and/or standard Schlenk techniques, unless otherwise stated. 4A molecular sieves were activated *in vacuo* at 180 °C for 24 h. Dry benzene and dichloromethane were purchased from Aldrich and were stored over activated 4A molecular sieves under nitrogen. Diethyl ether and tetrahydrofuran (THF) were first sparged with nitrogen and then dried by passage through activated alumina columns. Pentane was first washed with conc. HNO_3/H_2SO_4 to remove olefins, stored over $CaCl_2$ and then passed through activated alumina columns. All deuterated solvents were sparged with nitrogen, dried over activated 4A molecular sieves and stored under nitrogen. ^{1}H and ^{13}C NMR spectra were recorded on Varian 400 MHz spectrometer (400 and 100.4 MHz, respectively). All NMR spectra were recorded at room temperature unless otherwise noted and were indirectly referenced to TMS using residual solvent signals as internal standards. GC−MS spectra were recorded on a Varian Saturn 2100T, elemental analyses were performed on a PerkinElmer PE2400 microanalyzer at Georgetown, and UV−vis spectra were recorded on a Cary 50 spectrophotometer. All EPR, SQUID magnetization, and X-ray characterization details may be found in the Supporting Information.

All reagents were obtained commercially unless otherwise noted and typically stored over activated 4A molecular sieves. Ethylbenzene was obtained from Acros and purified by passing each through activated alumina. The neutral β-diketimine H[Cl_2NN][36] and corresponding copper catalyst {[Cl_2NN]Cu}$_2$(μ-benzene)[7] were prepared by literature methods or may be obtained from Strem Chemicals. [Cl_2NN]Cu-O^{t}Bu[23] and Gomberg's dimer [Ph_3C]$_2$ were prepared by a slight variation of literature procedures[37](see Supporting Information).

Preparation of Compounds. *[Cl_2NN]Cu-NHAr^{Cl3} (4).* To a suspension of [Cl_2NN]Cu-O^{t}Bu (0.114 g, 0.22 mmol) in ca. 8 mL of *n*-pentane was added 2,4,6-trichloroaniline (0.043 g, 0.22 mmol). The suspension turned intense blue solution and was stirred for 5 min at RT then the solvent was removed *in vacuo*. The remaining solid was extracted with 10 mL of *n*-pentane and filtered through Celite. The solution was then concentrated to 5 mL and allowed to stand overnight at −35 °C to yield blue crystals (0.087 g) in 62% yield. λ_{max} (ethylbenzene) = 741 nm (ε = 4480 M^{-1} cm^{-1}). Anal. Calcd for $C_{23}H_{16}Cl_7CuN_3$: C, 42.76; H, 2.50; N, 6.50. Found: C, 43.12; H, 2.35; N, 6.32.

{[Cl_2NN]Cu}$_2$(μ-NHAr^{F6})$_2$ (5). To a suspension of [Cl_2NN]Cu-O^{t}Bu (0.115 g, 0.22 mmol) in ca. 8 mL of *n*-pentane was added 3,5-bis(trifluoromethyl)aniline (0.0342 mL, 0.22 mmol). The suspension turned into an intense navy solution and was stirred for 5 min at RT, and then the solvent was removed *in vacuo*. The remaining solid was extracted with 10 mL of *n*-pentane and filtered through Celite. It was then concentrated to 5 mL and allowed to stand overnight at −35 °C to yield navy crystals (0.078 g) in 53% yield. λ_{max} (ethylbenzene) = 731 nm (ε = 3740 M^{-1} cm^{-1}). Anal. Calcd for $C_{25}H_{17}Cl_4CuF_6N_3$: C, 44.24; H, 2.52; N, 6.19. Found: C, 44.59; H, 2.21; N, 6.02.

[Cl_2NN]Cu(κ^2-NH-2-py) (6). To a suspension of [Cl_2NN]Cu-O^{t}Bu (0.114 g, 0.22 mmol) in ca. 8 mL of *n*-pentane was added 2-aminopyridine (0.021 g, 0.22 mmol). The suspension turned into a green solution and was stirred for 5 min at RT, and then the solvent was removed *in vacuo*. The remaining solid was extracted with 5 mL of Et_2O, filtered through Celite, then concentrated to 2 mL, layered with 1 mL of pentane, and then allowed to stand overnight at −35 °C to yield green crystals (0.030 g) in 25% yield. λ_{max} (ethylbenzene) = 664 nm (ε = 230 M^{-1} cm^{-1}). Anal. Calcd for $C_{22}H_{18}Cl_4CuN_4$: C, 48.59; H, 3.34; N, 10.30. Found: C, 48.44; H, 3.17; N, 9.97.

Catalytic Amination Ethylbenzene and Cyclohexane. A solution was prepared under inert atmosphere employing 1.0 mmol of H_2NAr^{Cl3}, H_2NAr^{F6}, or NH_2-2-py (1.0 equiv) along with 1.20 mmol of DTBP (1.2 equiv) in 20 mL of C-H substrate (ethylbenzene or cyclohexane). To this solution was added 1 mol % [Cl_2NN]Cu from a stock solution of the catalyst (0.100 mL = 0.01 mmol [Cl_2NN]Cu). The reactions were stirred inside a sealed pressure vessel at 90 °C for 24 h. Afterward the reaction mixture was allowed to cool, filtered through Celite, and analyzed by GC−MS and ^{1}H NMR after adding 1.0 mmol of 1,2,4,5-tetrachlorobenzene as a standard. Product characterization these substrates is found in the Supporting Information.

Stoichiometric Reaction of [Cl_2NN]Cu-NHAr with Ethylbenzene. Stock solutions of the copper(II) anilides were prepared by dissolving each of [Cl_2NN]Cu-NHAr^{Cl3} (32 mg, 0.050 mmol), [Cl_2NN]Cu-NHAr^{F6} (34 mg, 0.050 mmol), and [Cl_2NN]Cu(κ^2-NH-2-py) (27 mg, 0.050 mmol) in 10.0 mL of ethylbenzene (5.00 mM). Stock solutions of [Cl_2NN]Cu-O^{t}Bu, ^{t}BuOO^{t}Bu, and the 1,2,4,5-tetrachlorobenzene standard were prepared by dissolving [Cl_2NN]Cu-O^{t}Bu (114.6 mg, 0.219 mmol) in 10.0 mL of ethylbenzene (0.0216 M), by mixing ^{t}BuOO^{t}Bu (11 mL, 0.060 mmol) in a total volume of 1.00 mL of ethylbenzene (0.100 M), or by dissolving 1,2,4,5-tetrachlorobenzene (216 mg, 1.00 mmol) in 10.0 mL of ethylbenzene (0.100 M). Three sets of reactions employing each species [Cl_2NN]Cu-NHAr were carried out in sealed pressure vessels at 80 °C for 24 h each in either (a) neat ethylbenzene, (b) neat ethylbenzene with 1.0 equiv of [Cl_2NN]Cu-O^{t}Bu, or (c) neat ethylbenzene with 0.6 equiv of ^{t}BuOO^{t}Bu. These reaction mixtures were prepared as follows: (a) 2.00 mL of 5.00 mM [Cl_2NN]Cu-NHAr and 0.100 mL of 0.100 M 1,2,4,5-tetrachlorobenzene diluted to total volume of 10.00 mL with ethylbenzene; (b) 2.00 mL of 5.00 mM [Cl_2NN]Cu-NHAr, 0.457 mL of 0.0216 M [Cl_2NN]Cu-O^{t}Bu, and 0.100 mL of 0.100 M 1,2,4,5-tetrachlorobenzene diluted to total volume of 10.00 mL with ethylbenzene; and (c) 2.00 mL of 5.00 mM [Cl_2NN]Cu-NHAr, 0.100 mL of 0.100 M DTBP, and 0.100 mL of 0.100 M 1,2,4,5-tetrachlorobenzene diluted to total volume of 10.00 mL with ethylbenzene. See Tables S1 and S2 in the Supporting Information for product characterization details.

Kinetic Analysis of the Reaction of [Cl_2NN]Cu-NHAr^{Cl3} with Ethylbenzene in the Presence of ^{t}BuOO^{t}Bu. A stock solution of [Cl_2NN]Cu-NHAr^{Cl3} in ethylbenzene was prepared by dissolving [Cl_2NN]Cu-NHAr^{Cl3} (41 mg, 0.063 mmol) in ethylbenzene and diluting to 10.00 mL. 0.250 mL of this solution was diluted to 3.00 mL of ethylbenzene in a cuvette to achieve 0.49 mM solution. The solution was thermostated in a UV−vis spectrometer to either 25.0 or 80.0 °C. After being held at the appropriate temperature for 5 min, 0.1 mL of a stock solution of ^{t}BuOO^{t}Bu (3.5 μL in 1.00 mL of ethylbenzene) was added to the cuvette. Kinetic analysis monitored the decay of [Cl_2NN]Cu-NHAr^{Cl3} at λ_{max} = 741 nm and growth of [Cl_2NN]Cu-O^{t}Bu at λ_{max} = 471 nm. Both decay of **4** and growth of **3** followed zero-order kinetics with rate constants of 1.2(2) × 10^{-8} s^{-1} and 1.1(2) × 10^{-8} s^{-1} at 25 °C, respectively (Figure S10 in the

Supporting Information). At 80 °C, the zero-order rate constants for decay of **3** and growth of **4** are 6.5(3) × 10^{-7} s^{-1} and 7.0(3) × 10^{-7} s^{-1}, respectively (Figure S11 in the Supporting Information).

Reaction of Gomberg's Dimer with [Cl_2NN]Cu-NH-2-py (6). A stock solution of Gomberg's dimer with an internal standard was prepared by dissolving $(Ph_3C)_2$·pentane (36 mg, 0.0644 mmol) and 1,2,4,5-tetrachlorobenzene (13.9 mg, 0.0644 mmol) in 3.00 mL of C_6D_6 (0.0215 M). A vial containing 0.500 mL of this stock solution (0.0107 mmol $(Ph_3C)_2$·pentane and 0.0107 mmol standard) was concentrated to dryness *in vacuo* to remove excess pentane. 2.0 equiv of [Cl_2NN]Cu(κ^2-NH-2-py) (11.7 mg, 0.0215 mmol) in 0.500 mL of C_6D_6 was added to the vial containing 1.0 equiv of $(Ph_3C)_2$ and then transferred to an NMR tube for measurement. An immediate color change was observed resulting in a yellow solution, and the ^{1}H NMR spectrum of this solution was taken after 20 min identifying [Cl_2NN]Cu and Ph_3C-NH-2-py in 78% yield each (Figure S12 in the Supporting Information). The formation of Ph_3C-NH-2-py was confirmed by its independent synthesis according to a literature method[38] and observing its resulting ^{1}H NMR spectrum in C_6D_6 in the presence of 1 equiv of [Cl_2NN]Cu (Figure S13 in the Supporting Information).

Computational Methods. All computations employed the Gaussian 09 program.[39] Hybrid quantum mechanics/molecular mechanics (QM/MM) calculations on full experimental chemical models utilize the BP86[40] density functional for the QM region in conjunction with the 6-311+G(d) Pople basis set, which is a triple-ζ basis set augmented by diffuse and polarization functions on main group elements, and an f-polarization function on copper. The classical MM region was modeled by the Universal Force Field[41] (UFF) and contained the 2,6-dichloropylphenyl and methyl substituents of the β-diketiminate ligand. The remainder of the complex and ligands, as well as substrate molecules, were modeled at the aforementioned BP86/6-311+G(d) level of theory. The ONIOM methodology of Svensson et al. was used for all QM/MM simulations.[42]

Open and closed shell species were modeled within the unrestricted and restricted Kohn–Sham formalisms, respectively. All geometry optimizations were conducted without symmetry constraint using gradient methods. The energy Hessian was evaluated at all stationary points to designate them as either minima or transition states at the pertinent levels of theory. Free energies collected in Table S4 in the Supporting Information are reported at 298.15 K and 1 atm and are calculated with unscaled vibrational frequencies.

Spin density calculations and plots for [Cl_2NN]Cu-NHAr (**4**–**6**) collected in Table 3 and illustrated in Figure 4 were generated with ADF[43] (ADF 2007.1 BP/ZORA/TZ2P(+)) by optimizing coordinates obtained above. Slater-type orbital (STO) basis sets employed for H, C, and N atoms were of triple-ζ quality augmented with two polarization functions (ZORA/TZ2P) while an improved triple-ζ basis set with two polarization functions (ZORA/TZ2P+) was employed for the Cu atom. Scalar relativistic effects were included by virtue of the zero order regular approximation (ZORA). The 1s electrons of C and N as well as the 1s–2p electrons of Cu were treated as frozen core.

■ ASSOCIATED CONTENT

Supporting Information

Complete synthetic and kinetics details, additional characterization data for compounds **4**–**6** including EPR spectra, computational methods, X-ray details with fully labeled thermal ellipsoid plots for **4**–**6**. The full citation for Gaussian 09. Crystallographic information in CIF format for compounds **4**–**6**. This material is available free of charge via the Internet at http://pubs.acs.org.

■ AUTHOR INFORMATION

Corresponding Authors

*thw@georgetown.edu

*t@unt.edu

Present Address

#Institute of Chemical Sciences, Heriot-Watt University, Edinburgh EH14 4AS, U.K.

Notes

The authors declare no competing financial interest.

■ ACKNOWLEDGMENTS

We are grateful to NSF (CHE-1012523 and CHE-1300774, T.H.W.; CHE-1057785, T.R.C.) for support of this work. K.M. acknowledges financial support from the Friedrich-Alexander-University (FAU) Erlangen-Nürnberg.

■ REFERENCES

(1) (a) Dauban, P.; Dodd, R. H. In *Amino Group Chemistry*; Ricci, A., Ed.; Wiley-VCH: Weinheim, 2008; pp 55–92. (b) Collet, F.; Lescot, C.; Liang, C.; Dauban, P. *Dalton Trans.* **2010**, *39*, 10401–10413. (c) Zalatan, D. N.; Du Bois, J. *Top. Curr. Chem.* **2010**, *292*, 347–378. (d) Zhang, X. P.; Lu, H. *Chem. Soc. Rev.* **2011**, *40*, 1899–1909.

(2) Collet, F.; Dodd, R. H.; Dauban, P. *Chem. Commun.* **2009**, 5061–5074.

(3) Berry, J. F. *Comments Inorg. Chem.* **2009**, *30*, 28–66.

(4) (a) Fiori, K. W.; Du Bois, J. *J. Am. Chem. Soc.* **2007**, *129*, 562–568. (b) Liang, C.; Collet, F.; Robert-Peillard, F.; Muller, P.; Dodd, R. H.; Dauban, P. *J. Am. Chem. Soc.* **2008**, *130*, 343–350. (c) Du Bois, J. *Org. Process Res. Dev.* **2011**, *15*, 758–762. (d) Au, S.-M.; Huang, J.-S.; Yu, W.-Y.; Fung, W.-H.; Che, C.-M. *J. Am. Chem. Soc.* **1999**, *121*, 9120–9132. (e) Leung, S. K.-Y.; Tsui, W.-M.; Huang, J.-S.; Che, C.-M.; Liang, J.-L.; Zhu, N. *J. Am. Chem. Soc.* **2005**, *127*, 16629–16640. (f) Au, S.-M.; Huang, J.-S.; Che, C.-M.; Yu, W.-Y. *J. Org. Chem.* **2000**, *65*, 7858–7864. (g) Harvey, M. E.; Musaev, D. G.; Du Bois, J. *J. Am. Chem. Soc.* **2011**, *133*, 17207–17216. (h) Liang, J.-L.; Yuan, S.-X.; Huang, J.-S.; Yu, W.-Y.; Che, C.-M. *Angew. Chem., Int. Ed.* **2002**, *41*, 3465–3468. (i) Milczek, E.; Boudet, N.; Blakey, S. *Angew. Chem., Int. Ed.* **2008**, *47*, 6825–6828. (j) Yu, X.-Q.; Huang, J.-S.; Zhou, X.-G.; Che, C.-M. *Org. Lett.* **2000**, *2*, 2233–2236.

(5) (a) Kwart, H.; Khan, A. A. *J. Am. Chem. Soc.* **1967**, *89*, 1951–1953. (b) Badiei, Y. M.; Krishnaswamy, A.; Melzer, M. M.; Warren, T. H. *J. Am. Chem. Soc.* **2006**, *128*, 15056–15057.

(6) Gephart, R. T., III; Warren, T. H. *Organometallics* **2012**, *31*, 7728–7752.

(7) Badiei, Y. M.; Dinescu, A.; Dai, X.; Palomino, R. M.; Heinemann, F. W.; Cundari, T. R.; Warren, T. H. *Angew. Chem., Int. Ed.* **2008**, *47*, 9961–9964.

(8) (a) Lebel, H.; Huard, K.; Lectard, S. *J. Am. Chem. Soc.* **2005**, *127*, 14198–14199. (b) Huard, K.; Lebel, H. *Chem.—Eur. J.* **2008**, *14*, 6222–6230.

(9) Zhang, J.; Chan, P. W. H.; Che, C.-M. *Tetrahedron Lett.* **2005**, *46*, 5403–5408.

(10) (a) King, E. R.; Hennessy, E. T.; Betley, T. A. *J. Am. Chem. Soc.* **2011**, *133*, 4917–4923. (b) Hennessy, E. T.; Betley, T. A. *Science* **2013**, *340*, 591–595.

(11) (a) Liu, Y.; Che, C.-M. *Chem.—Eur. J.* **2010**, *16*, 10494–10501. (b) Wang, Z.; Zhang, Y.; Fu, H.; Jiang, Y.; Zhao, Y. *Org. Lett.* **2008**, *10*, 1863–1866.

(12) (a) Lyaskovskyy, V.; Olivos Suarez, A. I.; Lu, H.; Jiang, H.; Zhang, X. P.; de Bruin, B. *J. Am. Chem. Soc.* **2011**, *133*, 12264–12273. (b) Caselli, A.; Gallo, E.; Fantauzzi, S.; Morlacchi, S.; Ragaini, F.; Cenini, S. *Eur. J. Inorg. Chem.* **2008**, 3009–3019. (c) Cenini, S.; Gallo, E.; Penoni, A.; Ragaini, F.; Tollari, S. *Chem. Commun.* **2000**, 2265–2266. (d) Lu, H.; Subbarayan, V.; Tao, J.; Zhang, X. P. *Organometallics* **2010**, *29*, 389–393. (e) Lu, H.; Tao, J.; Jones, J. E.; Wojitas, L.; Zhang, X. P. *Org. Lett.* **2010**, *12*, 1248–1251. (f) Ruppel, J. V.; Kamble, R. M.; Zhang, X. P. *Org. Lett.* **2007**, *9*, 4889–4892.

(13) (a) Díaz-Requejo, M. M.; Belderraín, T. R.; Nicasio, M. C.; Trofimenko, S.; Pérez, P. J. *J. Am. Chem. Soc.* **2003**, *125*, 12078–12079. (b) Fructos, M. R.; Trofimenko, S.; Días-Requejo, M. M.; Pérez, P. J. *J. Am. Chem. Soc.* **2006**, *128*, 11784–11791. (c) Hamilton,

C. W.; Laitar, D. S.; Sadighi, J. P. *Chem. Commun.* **2004**, 1628−1629. (d) Liu, X.; Zhang, Y.; Wang, L.; Fu, H.; Jiang, Y.; Zhao, Y. *J. Org. Chem.* **2008**, *73*, 6207−6212. (e) Vedernikov, A. N.; Caulton, K. G. *Chem. Commun.* **2004**, 162−163.

(14) (a) Reed, S. A.; Mazzotti, A. R.; White, M. C. *J. Am. Chem. Soc.* **2009**, *131*, 11701−11706. (b) Liu, G.; Yin, G.; Wu, L. *Angew. Chem.* **2008**, *120*, 4811−4814. (c) Liu, G.; Yin, G.; Wu, L. *Angew. Chem., Int. Ed.* **2008**, *47*, 4733−4736.

(15) Shimizu, Y.; Obora, Y.; Ishii, Y. *Org. Lett.* **2010**, *12*, 1372−1374.

(16) Jordan-Hore, J. A.; Johansson, C. C. C.; Gulias, M.; Beck, E. M.; Gaunt, M. J. *J. Am. Chem. Soc.* **2008**, *130*, 16184−16186.

(17) (a) Smith, K.; Hupp, C. D.; Allen, K. L.; Slough, G. A. *Organometallics* **2005**, *24*, 1747−1755. (b) Pelletier, G.; Powell, D. A. *Org. Lett.* **2006**, *8*, 6031−6034. (c) Powell, D. A.; Fan, H. *J. Org. Chem.* **2010**, *75*, 2726−2729. (d) Shuai, Q.; Deng, G.; Chua, Z.; Bohle, D. S.; Li, C.-J. *Adv. Synth. Catal.* **2010**, *352*, 632−636.

(18) Tran, B. L.; Li, B.; Driess, M.; Hartwig, J. F. *J. Am. Chem. Soc.* **2014**, *136*, 2555−2563.

(19) (a) Ramirez, T. A.; Zhao, B.; Shi, Y. *Chem. Soc. Rev.* **2012**, *41*, 931−942. (b) Clark, J. S.; Roche, C. *Chem. Commun.* **2005**, 5175−5177.

(20) (a) Davies, H. M. L.; Manning, J. R. *Nature* **2008**, *451*, 417−424. (b) Godula, K.; Sames, D. *Science* **2006**, *312*, 67−72. (c) Wehn, P. M.; Du Bois, J. *Angew. Chem., Int. Ed.* **2009**, *48*, 3802−3805.

(21) Aguila, M. J. B.; Badiei, Y. M.; Warren, T. H. *J. Am. Chem. Soc.* **2013**, *135*, 9399−9406.

(22) Evans, R. E.; Zbieg, J. R.; Zhu, S.; Li, W.; Macmillan, D. W. C. *J. Am. Chem. Soc.* **2012**, *135*, 16074−16077.

(23) Wiese, S.; Badiei, Y. M.; Gephart, R. T.; Mossin, S.; Varonka, M. S.; Melzer, M. M.; Meyer, K.; Cundari, T. R.; Warren, T. H. *Angew. Chem., Int. Ed.* **2010**, *49*, 8850−8855.

(24) Gephart, R. T.; Huang, D. L.; Aguila, M. J. B.; Schmidt, G.; Shahu, A.; Warren, T. H. *Angew. Chem., Int. Ed.* **2012**, *51*, 6488−6492.

(25) Melzer, M. M.; Mossin, S.; Dai, X.; Bartell, A. M.; Kapoor, P.; Meyer, K.; Warren, T. H. *Angew. Chem., Int. Ed.* **2010**, *122*, 904−907.

(26) Dai, X.; Warren, T. H. *Chem. Commun.* **2001**, 1998−1999.

(27) (a) Kempe, R. *Eur. J. Inorg. Chem.* **2003**, 791−803. (b) Deeken, S.; Motz, G.; Kempe, R. *Z. Anorg. Allg. Chem.* **2007**, *633*, 320−325.

(28) (a) van Albada, G. A.; Smeets, W. J. J.; Veldman, N.; Spek, A. L.; Reedijk, J. *Inorg. Chim. Acta* **1999**, *290*, 105−112. (b) Comba, P.; Curtis, N. F.; Lawrance, G. A.; Sargeson, A. M.; Skelton, B. W.; White, A. H. *Inorg. Chem.* **1986**, *25*, 4260−4267.

(29) Luo, Y.-R. *Handbook of Bond Dissociation Energies in Organic Compounds*; CRC Press: Boca Raton, FL, 2002.

(30) Gephart, R. T.; McMullin, C. L.; Sapiezynski, N. G.; Jang, E. S.; Aguila, M. J. B.; Cundari, T. R.; Warren, T. H. *J. Am. Chem. Soc.* **2012**, *134*, 17350−17353.

(31) Finn, M.; Friedline, R.; Suleman, N. K.; Wohl, C. J.; Tanko, J. M. *J. Am. Chem. Soc.* **2004**, *126*, 7578−7584.

(32) Warren, J. J.; Tronic, T. A.; Mayer, J. M. *Chem. Rev.* **2010**, *110*, 6961−7001.

(33) (a) Kharasch, M. S.; Sosnovsky, G. *J. Am. Chem. Soc.* **1958**, *80*, 756−756. (b) Kharasch, M. S.; Sosnovsky, G.; Yang, N. C. *J. Am. Chem. Soc.* **1959**, *81*, 5819−5824. (c) Rawlingson, D. J.; Sosnovsky, G. *Synthesis* **1972**, 1−28. (d) Andrus, M. B.; Lashley, J. C. *Tetrahedron* **2002**, *58*, 845−866.

(34) Eames, J.; Watkinson, M. *Angew. Chem., Int. Ed.* **2001**, *40*, 3567−3571.

(35) (a) Kochi, J. K. *Science* **1967**, *155*, 415−424. (b) Jenkins, C. L.; Kochi, J. K. *J. Am. Chem. Soc.* **1972**, *94*, 856−865. (c) Kochi, J. K.; Jenkins, C. L. *J. Org. Chem.* **1971**, *36*, 3095−3102. (d) Kochi, J. K.; Subramanian, R. V. *J. Am. Chem. Soc.* **1965**, *87*, 1508−1514.

(36) Budzelaar, P. H. M.; Moonen, N. N. P.; de Gelder, R.; Smits, J. M. M.; Gal, A. W. *Eur. J. Inorg. Chem.* **2000**, 753−769.

(37) Gomberg, M. *J. Am. Chem. Soc.* **1900**, *22*, 757−771.

(38) Zunszain, P. A.; Shah, M. M.; Miscony, Z.; Javadzadeh-Tabatabaie, M.; Haylett, D. G.; Ganellin, C. R. *Arch. Pharm.* **2002**, *335*, 159−166.

(39) Frish, M. J.; et al. *Gaussian 09, Revision A.1*; Gaussian, Inc: Wallingford, CT, 2009 (full citation in the Supporting Information).

(40) (a) Becke, A. D. *Phys. Rev. A* **1988**, *38*, 3098−3100. (b) Perdew, J. P. *Phys. Rev. B* **1986**, *33*, 8822−8824.

(41) Rappé, A. K.; Casewit, C. J.; Colwell, K. S.; Goddard, W. A. I.; Skiff, W. M. *J. Am. Chem. Soc.* **1992**, *114*, 10024−10035.

(42) Svensson, M.; Humbel, S.; Froese, R. D. J.; Matsubara, T.; Sieber, S.; Morokuma, K. *J. Phys. Chem.* **1996**, *100*, 19357−19363.

(43) (a) te Velde, G.; Bickelhaupt, F. M.; Baerends, E. J.; Fonseca Geurra, C.; Snijders, J. G.; Ziegler, T. *J. Comput. Chem.* **2001**, *22*, 931−967. (b) Fonseca Geurra, C.; Snijders, J. G.; te Velde, G.; Baerends, E. J. *J. Theor. Chem. Acc.* **1998**, *99*, 391−403.